



MINING ROCK PROPERTIES. ROCK MECHANICS AND GEOPHYSICS

Research paper

<https://doi.org/10.17073/2500-0632-2022-07-11>


UDC 622.83:550.83



Influence of random parameter joint length on rock electrical conductivity

P. E. Sizin , A. S. Voznesenskii , L. K. Kidima-Mbombi 

University of Science and Technology MISIS, Moscow, Russian Federation

 al48@mail.ru

Abstract

Rock joint hollowness coefficient is an important parameter when resolving practical mining problems. Geophysical methods used to resolve this problem are indirect. Thus the interpretation of their results may cause certain difficulties as a result of the uncertainty of the physical relationships between the parameters of joints and the measurement results. One of the ways to resolve this problem is to combine experimental research methods with analytical and numerical simulation. The studies were aimed at investigating the electrical conductivity of a two-dimensional medium in the presence of thin insulating (non-conducting) joints. This paper proposes an analytical method for assessing the dependence of the specific conductivity of a medium with inclusions in the form of elliptical joints on their half-length. This dependence is shown to have the form of an exponent depending on the square of the length of the maximum semi-axis as an argument. The simulation method is based on the assumption of the elliptical shape of a joint when the length of the minor semi-axis of the ellipses tends to zero. A review of publications and their results presented in this paper showed that this method for determining the specific conductivity of the medium with thin joints is one of the best in terms of compliance with experimental data. Its predictions are close to those of the Effective Media Approximation (EMA). However, the proposed method is distinguished by the simplicity of the formulas and their physical visibility essential for the use in interpreting the data of a physical experiment. In two-dimensional formulation, numerical simulation of the specific electrical conductivity of a sample of a medium measuring 1×1 m with elliptical joints of conductivity less than that of the matrix was carried out in the COMSOL Multiphysics environment. A square sample of unit sizes with unit conductivity was considered in which 25 joints with uniform distribution along the length occurred. 40 models were built wherein the maximum length of the joints varied from 0.01 to 0.4 sample size in increments of 0.01 m. The satisfactory concordance of the results of numerical and analytical models, both visual and confirmed by statistical estimates, has been shown. It was noted that when the size of the joints changes to achieve the value of the maximum semi-axis $a = 0.15$ m, the influence of single joints that do not extend beyond the boundaries of the sample prevails. Above this value, at $a > 0.15$ m, the influence of joint coalescence, as well as their extension to and beyond the sample boundaries begins to affect. Comparison of the proposed theoretical model of electrical conductivity, depending on the square of the length of the maximum semi-axis of a joint, with a similar model in the form of an exponent with a linear dependence showed a better concordance of the proposed model with observations at the stage of the lack of joint coalescence and their extension to the sample boundaries at $a < 0.15$ m. At $a > 0.15$ m. The proposed model has a lower coefficient of determination compared to the full range including both intervals, but higher than that of the model with a linear dependence in the exponent argument. This indicates the universal nature of the proposed model.

Keywords

electrical resistance, joint length, numerical, analytical, simulation, COMSOL Multiphysics

For citation

Sizin P.E., Voznesenskii A.S., Kidima-Mbombi L.K. Influence of random parameter joint length on rock electrical conductivity. *Mining Science and Technology (Russia)*. 2023;8(1):30–38. <https://doi.org/10.17073/2500-0632-2022-07-11>


СВОЙСТВА ГОРНЫХ ПОРОД. ГЕОМЕХАНИКА И ГЕОФИЗИКА

Научная статья

Влияние длины трещин со случайными параметрами на электрическую проводимость горных пород

П. Е. Сизин , А. С. Вознесенский , Л. К. Кидима Мбомби 

Университет науки и технологий МИСИС, г. Москва, Российская Федерация

 al48@mail.ru

Аннотация

При решении практических задач горного производства возникает необходимость оценки трещинной пустотности горных пород. Геофизические методы при решении данной задачи являются косвенными, поэтому интерпретация результатов может вызывать определенные трудности, обу-



словленные непрозрачностью физических связей между параметрами трещин и результатами измерений. В этой связи одним из путей решения данной проблемы является сочетание экспериментальных методов исследования с аналитическим и численным моделированием. Исследования были направлены на изучение электрической проводимости двумерной среды при наличии тонких изолирующих трещин. В статье предложен аналитический метод оценки зависимости удельной проводимости среды с включениями в виде эллиптических трещин от их полудлины. Показано, что данная зависимость имеет вид экспоненты, зависящей от квадрата длины максимальной полуоси в качестве аргумента. Метод моделирования основан на допущении эллиптической формы трещины при устремлении к нулю длины малой полуоси эллипсов. Анализ публикаций и результаты, изложенные в статье, показали, что такой метод нахождения удельной проводимости среды с тонкими трещинами один из наилучших в плане соответствия экспериментальным данным. Его предсказания близки к предсказаниям метода эффективной среды (ЕМА), но он отличается простотой формул и их физической наглядностью, что существенно для использования при интерпретации данных физического эксперимента. В двумерной постановке проведено численное моделирование в среде COMSOL Multiphysics удельной электрической проводимости образца среды размером 1×1 м с эллиптическими трещинами меньшей, чем у матрицы, проводимости. Рассмотрен квадратный образец единичных размеров с единичной проводимостью, в котором помещалось 25 трещин, имевших равномерное распределение по длине. Было построено 40 моделей, в которых максимальная длина трещин менялась от 0,01 до 0,4 размера образца, с шагом 0,01 м. Показано удовлетворительное соответствие результатов численной и аналитической моделей как визуальное, так и подтвержденное с помощью статистических оценок. Отмечено, что при изменении размера трещин до значения максимальной полуоси $a = 0,15$ м преобладает влияние одиночных трещин, не выходящих за границы образца. Выше этого значения при $a > 0,15$ м начинает сказываться влияние слияния трещин, а также их выхода на границы и за пределы образца. Сравнение предложенной теоретической модели электрической проводимости, зависящей от квадрата длины максимальной полуоси трещины, с похожей моделью в виде экспоненты с линейной зависимостью показало лучшее соответствие предложенной модели на стадии отсутствия слияния трещин и их выхода на границы образца при $a < 0,15$ м. При $a > 0,15$ м предложенная модель имеет меньший коэффициент детерминации по сравнению с полным диапазоном, включающим оба участка, но более высокий, чем у модели с линейной зависимостью в аргументе экспоненты, что говорит об универсальном характере предложенной модели.

Ключевые слова

электрическое сопротивление, длина трещины, численный, аналитический, моделирование, COMSOL Multiphysics

Для цитирования

Sizin P.E., Voznesenskii A.S., Kidima-Mbombi L.K. Influence of random parameter joint length on rock electrical conductivity. *Mining Science and Technology (Russia)*. 2023;8(1):30–38. <https://doi.org/10.17073/2500-0632-2022-07-11>

Introduction

The relevance of the problem of assessing rock joint hollowness coefficient emerges from the need to address problems of strength [1–4] and stability of rocks around mine workings [5–7], hydraulic fracturing of rock mass [8–10], fluid filtration through a rock mass [11, 12], the calculation of drilling and blasting parameters [13–15], as well as other practical problems of mining. Geological [16–18], surveying [19–21], video methods [22, 23] are used to determine rock jointing. A special place here is occupied by geophysical methods [24–26]. A significant place is given to electromagnetic [27] and electric [28] methods. Despite the significant advantages of electrical methods for studying rock jointing, they also have a number of disadvantages. The geophysical methods are indirect, so the interpretation of their results may cause certain difficulties due to the uncertainty of the physical relationships between the parameters of joints and the measurement results. In this regard, one

of the ways of resolving this problem is to combine experimental research methods with analytical and numerical simulation. As an example, we can cite study [29] which shows the theoretical feasibility of analytical calculation of the relationship between rock jointing and electrical resistance.

The problem of sample resistance with joints ultimately comes down to the problem of the conductivity of a two-component medium consisting of a continuum (matrix) and a component represented by individual inclusions. At low concentration of the inclusions, such conductivity is easily calculated [30]. It is connected with the concentration of inclusions according to the linear law. In the case of high concentrations, the best method is considered to be the Effective Media Approximation (EMA) [31–33]. Initially designed for “volumetric” inclusions (spheres in three-dimensional space, circles, squares, etc. in two-dimensional problems), it was then modified for the case of “disembodied” inclusions, such as infinitely thin disks in the



three-dimensional case and “scratches” in the two-dimensional case [34]. This approach enables the electrical conductivity of rocks containing joints to be simulated. At the same time, in actual rocks, joints can be empty or containing low-conducting liquids (oil). They can also be filled with a solution of salts (high-conductive fluid) [35]. In the former case, the joints should be considered insulating, while in the latter one, almost perfectly conductive when the fluid conductivity is several orders of magnitude higher than the conductivity of the host rock [29]. In this paper, a model of “dry” or fluid-filled joints with a conductivity of 10-4 of the conductivity of a rock matrix is used. It should also be noted that at some rather high concentration of inclusions, coalescence occurs when they overlap, forming a continuous conductive or insulating cluster [36–38]. However, in the first place, such high concentrations of joints will not be considered, since when approaching the coalescence threshold, disintegration of a sample occurs.

The purpose of this study is to develop analytical and numerical models of the dependencies of the electrical resistance of a rock sample on the size of joints, and compare the results of simulating by these methods with each other, as well as with the results of testing rock samples.

2. Research techniques

2.1. Analytical method

Let us consider the problem of conductivity of a two-dimensional medium with thin joints (in the limit, scratches of zero thickness). For the case of low concentration of scratches perpendicular to the gradient of the applied voltage (and the direction of the electric current), we get [34]

$$\sigma = \sigma_0 \left(1 - \pi \left(\frac{l}{2} \right)^2 N \right), \quad (1)$$

where σ_0 is conductivity of a medium without joints; $l/2$ is the “radius” of a joint, equal to half of its length; N is two-dimensional concentration of joints. In the case of chaotic orientation of the joints (uniform distribution by angle), the contribution of these joints to the conductivity is halved:

$$\sigma = \sigma_0 \left(1 - \frac{\pi l^2}{8} N \right).$$

The reason is that when the conductivity is averaged by a statistical ensemble of joints, one of the two coordinate axes does not make a contribution: the insulating joints oriented parallel to the current do not significantly affect conductivity.

Note that if there is exactly a single joint in a square sample with a side L and a conductivity of σ_0 , perpendicular to the field, the concentration $N = 1/L^2$, and the sample conductivity is:

$$\sigma = \sigma_0 \left(1 - \frac{\pi l^2}{4L^2} \right).$$

Let us suppose now a square sample with a side L contains n joints perpendicular to the applied voltage and has a conductivity of σ . Let us place another similar joint into this sample. In this case, the increment of the sample conductivity

$$\Delta\sigma = -\sigma \frac{\pi l^2}{4L^2}.$$

Thus, we obtain a differential equation ($\Delta n = 1$)

$$\frac{\Delta\sigma}{\Delta n} = -\sigma \frac{\pi l^2}{4L^2}, \quad (2)$$

the solution of which is

$$\sigma = \sigma_0 e^{-\frac{\pi l^2}{4L^2} n},$$

where the obvious initial condition is used: the conductivity in the absence of joints is σ_0 . Given the two-dimensional concentration of joints, this solution can be written in the form:

$$\sigma = \sigma_0 e^{-\frac{\pi l^2}{4} N}. \quad (3)$$

Let the lengths of the joints now be distributed evenly in the range from 0 to l . In this case, the average value of the square of the joint length is $l^2/3$. This value will determine the average contribution of an individual joint to the change in conductivity. Then the initial differential equation should be replaced with

$$\frac{\Delta\sigma}{\Delta n} = -\sigma \frac{\pi l^2}{12L^2},$$

and we get for the sample conductivity

$$\sigma = \sigma_0 e^{-\frac{\pi l^2}{12L^2} n},$$

or taking into account the concentration of joints in the two-dimensional case $N = n/L^2$

$$\sigma = \sigma_0 e^{-\frac{\pi l^2}{12} N}. \quad (4)$$

It is often beneficial to use half the length of a joint $a = l/2$ (similar to the radius of a circular inclusion), and then

$$\sigma = \sigma_0 e^{-\frac{\pi a^2}{3} N}. \quad (5)$$

If we denote $A = \pi N/3$, formula (3) takes on form

$$\sigma = e^{-Aa^2}. \quad (6)$$

The parameter A has the physical meaning of the effective concentration of joints and can be found from a numerical simulation or a physics experiment.

It should be noted that in [36], use of the EMA method for conductivity of a two-dimensional medium with parallel insulating joints, the following expression was obtained:

$$\sigma = \sigma_0 \left(\sqrt{1 + \frac{1}{4} \left(\frac{\pi l^2}{4} N \right)^2} - \frac{1}{2} \frac{\pi l^2}{4} N \right)^2. \quad (7)$$

This expression at not very high concentrations of joints, up to

$$\frac{\pi l^2}{4} N \approx 1,$$

is very close to (3), but (3) is much simpler, more convenient for analysis, and has a quite transparent physical meaning.

2.2. Numerical method

The methodology for constructing geometry and setting the properties and boundary conditions of a model when using this method is explained in [39]. A feature of this approach was the construction of geometry, properties, and boundary conditions of the model using program scripts. Changing the joint parameters in each specific model was achieved by changing the values of the variables used to set the length, position, and the angle of inclination of the ellipses which simulated the joints. These parameters were changed within the specified limits using a random number generator with a uniform distribution.

The simulation was carried out using the COMSOL Multiphysics environment in conjunction with Matlab. The script was written and the changes were made in accordance with the required joint parameters. Figure 1 shows a drawing of one of the models as an example. The simulation was carried out in dimensionless relative units. Since the results for electrical conductivity and resistance are most conveniently represented in relative values, the following technique was used in the simulation. A rock sample was selected in the form of a square with a side of 1 m, with a specific conductivity of 1 Cm/m. A voltage of 1 V was applied to the two opposite sides. In the absence of joints, the current in the sample was 1 A. When joints were added, the current became less than 1 A. By virtue of Ohm's law, numerically coinciding with both the conductivity and the specific conductivity of a fractured rock.

A total of 40 models were used when changing the half-lengths of the joints from 0.01 to 0.4 m. One

more model was jointless and corresponded to the case $a/2 = 0$. The minor semi-axis of the joints was 0.01 m, and the major semi-axis in accordance with the uniform distribution varied from 0.01 m to the value assigned in the series of experiments, ranging from 0.01 to 0.4 m. The joint angle varied within $\pm 20^\circ$. The number of joints in the sample was 25. The maximum displacements of the centers of the ellipses from the regular grid horizontally and vertically with their uniform distribution amounted to $\pm 0.2DX$ and $\pm 0.5DY$, respectively, where DX , DY were the average distances between the centers of joints along X and Y axes, respectively. With some combinations of joint sizes and displacements relative to their centers, they could partially or completely extend beyond the contour of a sample, while their total number was less than the specified value. In addition, the coalescence of joints led to a decrease in their equivalent number. Several interconnected joints led to an effect equivalent to the effect of one joint of greater length. The specific conductivity of the rock matrix was 1 cm/m, and that of the joint material, 10–4 cm/m. The boundary conditions were as follows: on the upper edge, the potential V was set at $V_0 = 1$ V, and on the lower edge $V_0 = 0$ V (“earth”). On the side edges, zero conductivity was set $\sigma = 0$ cm/m (insulation).

For finding solutions in the COMSOL Multiphysics system, a static problem solver was used in the simulation, which allowed obtaining the distribution of currents and voltages in steady state.

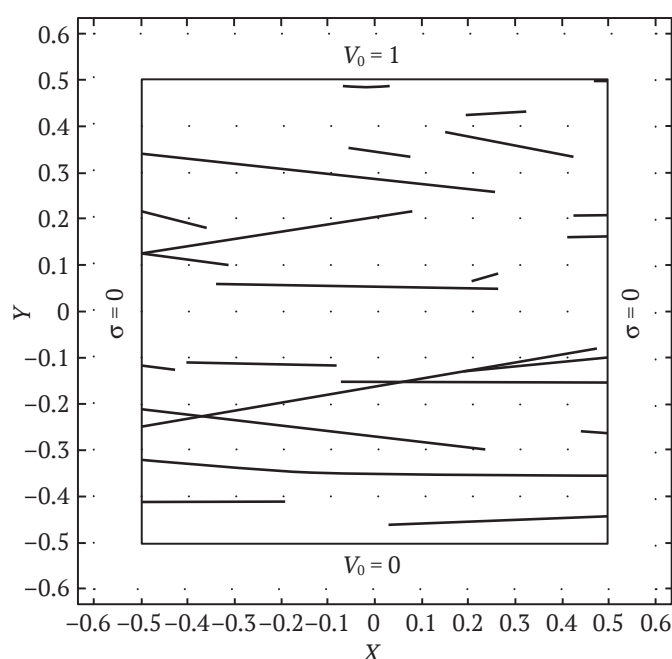


Fig. 1. Example of a 2D model scheme for a numerical experiment

3. Findings

Figure 2 presents examples of the results of simulation of current flow through a sample without joints (*a*), with elliptical joints of half-length from 0.01 to 0.1 m (*b*), from 0.01 to 0.2 m (*c*), from 0.01 to 0.5 m (*d*). The red current lines clearly demonstrate the effect of joints, acting as “dams” for current.

On the graph in Fig. 3, the sample conductivity dependencies obtained by finite element calculations are represented in the form of separate points. The formula (6) was used to approximate the results obtained.

As can be seen the satisfactory mutual convergence of the theoretical and experimental attracts them to each other. The quantitative estimates of this convergence are given below.

4. Findings Discussion

If there are no joints in a sample, the current lines (Fig. 2, *a*) are evenly distributed over the sample along its horizontal axis, and the electrical potential demonstrates a uniform change along the vertical axis. In the graph in Fig. 3, this case corresponds to the joint half-length $a/2 = 0$. The presence of joints of horizontal direction in Fig. 2, *b* increases the length of the current lines. This is the reason for the decrease in conductivity with an increase in $a/2$. With a significant increase in the joints length up to the complete intersection of the sample in Fig. 2, *e*, the length of the current lines increases significantly with a significant change in their configuration as compared to the intact sample in Fig. 2, *a*. In this

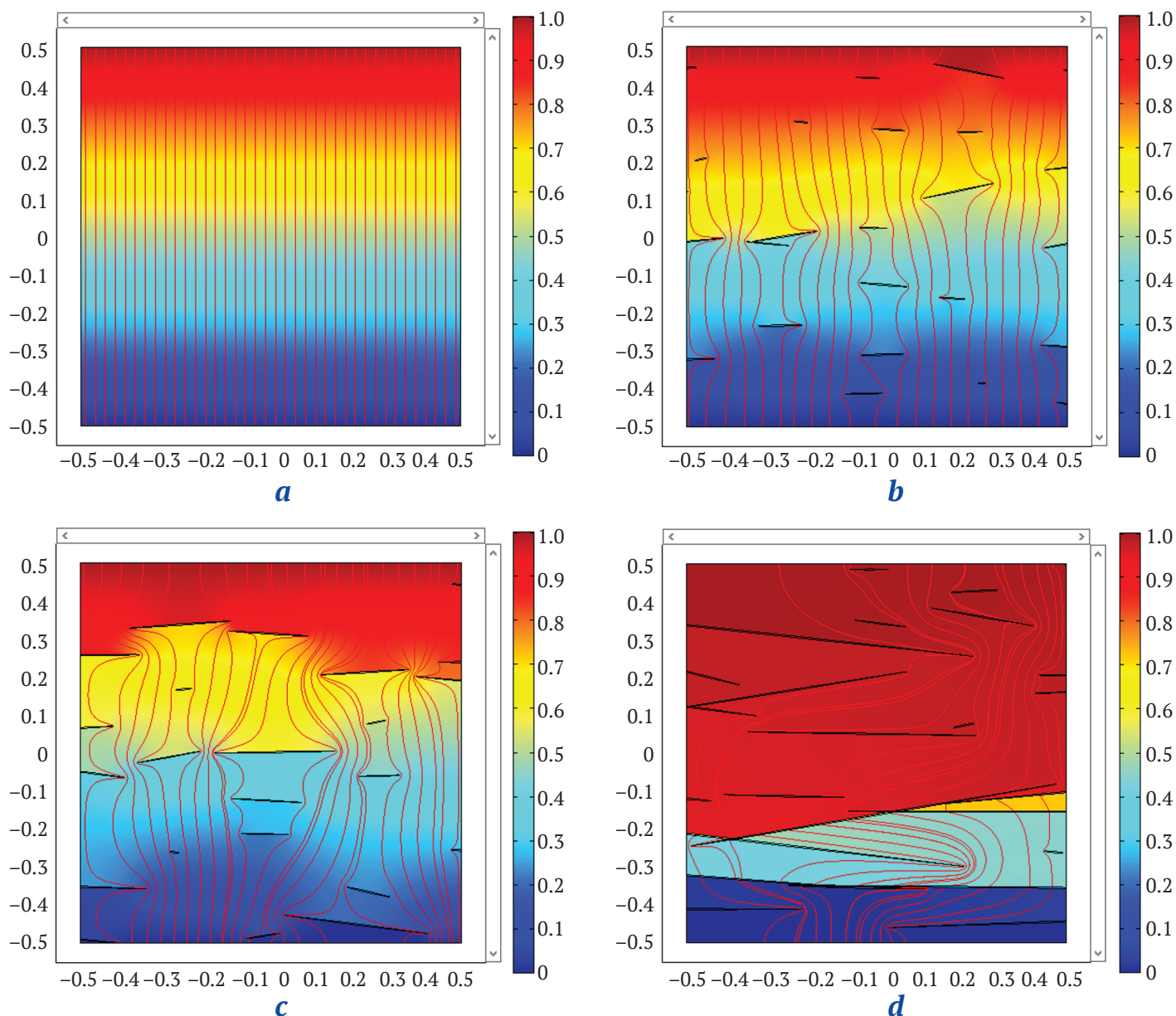


Fig. 2. Current lines (red lines) and the distribution of electrical potential relative to the lower boundary according to the scales on the right

case, the electric potential demonstrates a jump-like change in the places of joints. Since the numerical model includes a probabilistic distribution of joint parameters, the experimental points in Fig. 3 have random deviations from the analytical curve. At the same time, up to the value of $a/2 = 0.15$ (m), the points are located closer to the analytical curve than with larger values of $a/2$. This is due to the fact that the extent of high-impedance joints beyond the boundaries of the sample begins to take effect also owing to their coalescence leading to significant curvatures of the current lines.

The experimental points are well described by dependency (6), in which the parameter A is selected using the Statistica package according to the least-squares criterion

$$y = \exp(-21.23x^2),$$

where $x = a/2$ is the maximum value of the major semi-axis of an elliptical joint. The value varied from 0.01 to 0.4; $y = \sigma/\sigma_0$ is the relative conductivity of the sample; σ_0 is the conductivity of the sample without joints. In this case, the parameter is $A = 21.33$, which corresponds to the equivalent number of joints $N_{eq} = 3A/\pi = 20.4$. This number is noticeably less than 25, the true number of joints in the sample. This is explained by the fact that with considerable sizes of joints, some of them merge with each other or occur on the boundaries of the sample. The determination coefficient of the numerical simulation results at approximation $R^2 = 0.977$, the root-mean-square deviation (RMSD) = 0.0494 cm/m, reflecting the random nature of the joint parameters and less than 10 % of the average conductivity value of 0.5 cm/m in the experiment. For the initial section of the curve, where the influence of edge effects and coalescence of joints does not affect, this value is much lower.

Accordingly, for a more detailed analysis, the whole range of joint half-length values a was divided into two sections: $0 \leq a < 0.15$ m (section 1) and $0.15 \leq a \leq 0.40$ m (section 2), for which statistical estimates were carried out separately.

It is interesting to compare the results obtained with the experimental results. In [40], the findings of the conductivity study for the Chayandinsky deposit reservoir rock samples are considered. The dependence of the change in specific electrical conductivity on the proportion of fracture porosity was approximated by an exponent

$$y = a_0 \exp(-a_1 x), \quad (8)$$

where a_0, a_1 are the exponential dependency parameters. The graph of the dependence according to formula (8) in comparison with the numerical simulation results is shown in Fig. 4. In this case, $a_0 = 1.179$; $a_2 = 5.251$.

As follows from the comparison of Fig. 4 with Fig. 3, visually, the approximation by dependence (8) is worse than that by dependence (6). If the experimental data curve in the first section is curved upwards, then the dependence (8) is curved downwards. In the second section, the curve (8) passes above the experimental points, although in this section the curvature of the course of both curves coincides.

Table 1 shows the results of approximation of the data obtained according to formulas (6) and (8). For formula (6), the values of parameter A and the calculated values of the equivalent number of joints N_{eq} are also given. It should be noted that the calculations according to formula (7) gave results close to the results of formula (6), so they are not given separately in Table 1. For formula (8), the values of parameter A were not calculated, because this model differed from model (6) in essence.

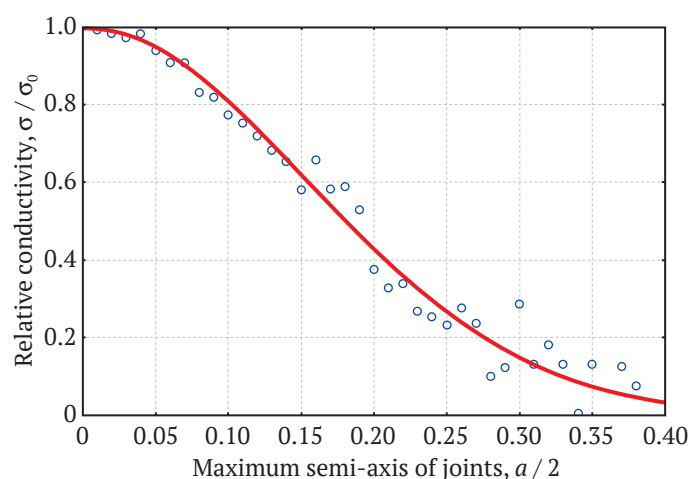


Fig. 3. Dependencies of sample conductivity on joint length obtained by a numerical method (hollow circles) and the approximation by formula (6) (solid line)

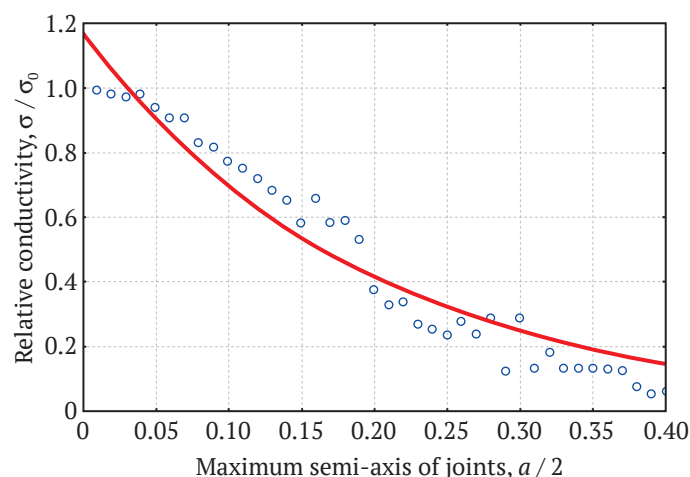


Fig. 4. Approximation of experimental points by dependence (8)

Table 1
Statistical parameters of numerical simulation results approximation according to formulas (6) and (8)

Formula number	Section	R^2	RMSD	A	N_{eq}
(6)	1+2	0.979	0.014	20.34	21.30
	1	0.987	0.00014	23.32	24.42
	2	0.901	0.016	19.96	20.90
(8)	1+2	0.935	0.044	–	–
	1	0.932	0.0036	–	–
	2	0.922	0.012	–	–

As follows from Table 1, formula (8) gives worse results compared to formula (6). Thus, for the complete curve (8) and for its first section, the determination coefficient R^2 is lower, and the RMSD is higher than for curve (6). For the second section, where joints overlap and their extension beyond the sample limits begin to affect, this difference is lower, but still significant.

In paper [40], the author explains that the dependence of type (8) is used to approximate joints in actual samples. Such samples have a rather developed system of joints, which in large part overlap with each other, and also demonstrate an extent beyond the sample. This factor is predominant in the description of the dependencies in question, and dependence (8) is acceptable for this case.

Thus, it can be concluded that formula (6) is acceptable for describing the relationship between the size of joints and the conductivity of a rock sample in the case of "dry" or low-conductive fluid-filled joints at their low concentration before the manifestation of joint coalescence phenomena.

Conclusion

1. An analytical method for assessing the dependence of the specific electrical conductivity of a medium with inclusions in the form of thin elliptical joints on their half-length is proposed. It was shown that this dependence has the form of an exponent depending on the square of the length of the maximum

semi-axis as an argument. The simulation method is based on the assumption of the elliptical shape of a joint when the length of the minor semi-axis of the ellipses tends to zero. The review of publications and the results presented in this paper showed that this method for determining the specific conductivity of the medium with thin joints is one of the best in terms of the compliance with experimental data. Its predictions are close to those of the Effective Media Approximation (EMA), while the proposed method is distinguished by the simplicity of the formulas and their physical visibility essential for use in interpreting the data of a physical experiment.

2. In a two-dimensional formulation, a numerical simulation of the specific electrical conductivity of a sample of a medium measuring 1×1 m with elliptical joints of conductivity less than that of the matrix was carried out using the COMSOL Multiphysics environment. Satisfactory concordance of the results of numerical and analytical models, both visual and confirmed by statistical estimates, was shown. It was noted that when the size of the joints changes to the value of the maximum semi-axis $a = 0.15$ m, the influence of single joints which do not extend beyond the boundaries of the sample prevails. Above this value, the influence of joint coalescence as well as their extension to and beyond the sample boundaries begins to affect.

3. Comparison of the proposed theoretical model of electrical conductivity, depending on the square of the length of the maximum semi-axis of an elliptical joint, with a similar model in the form of an exponent with a linear dependence on the half-length of a joint showed a better concordance of the proposed model with the observations at the stage of the lack of joint coalescence and their extension to the sample boundaries at $a < 0.15$ m. At $a > 0.15$ m, the proposed model has a lower coefficient of determination compared to the full range including both intervals, but higher than that of the model with a linear dependence in the exponent argument. This indicates the universal nature of the proposed model.

References

1. Feng P., Zhao J., Dai F. et al. Mechanical behaviors of conjugate-flawed rocks subjected to coupled static–dynamic compression. *Acta Geotechnica*. 2022;17(5):1765–1784. <https://doi.org/10.1007/s11440-021-01322-6>
2. Feng P., Dai F., Shuai K. et al. Dynamic mechanical behaviors of pre-fractured sandstone with noncoplanar and unparallel flaws. *Mechanics of Materials*. 2022;166:104219. <https://doi.org/10.1016/j.mechmat.2022.104219>
3. Yan Z., Dai F., Liu Y. et al. Experimental investigation of pre-flawed rocks under combined static-dynamic loading: Mechanical responses and fracturing characteristics. *International Journal of Mechanical Sciences*. 2021;211:106755. <https://doi.org/10.1016/j.ijmecsci.2021.106755>
4. Qi C., Xia C., Dyskin A. et al. Effect of crack interaction and friction on the dynamic strength of rock-like materials with many cracks. *Engineering Fracture Mechanics*. 2021;257:108006. <https://doi.org/10.1016/j.engfracmech.2021.108006>



5. Gao M., Xie J., Gao Y. et al. Mechanical behavior of coal under different mining rates: A case study from laboratory experiments to field testing. *International Journal of Mining Science and Technology*. 2021;31(5):825–841. <https://doi.org/10.1016/j.ijmst.2021.06.007>
6. Lu J., Jiang C., Jin Z. et al. Three-dimensional physical model experiment of mining-induced deformation and failure characteristics of roof and floor in deep underground coal seams. *Process Safety and Environmental Protection*. 2021;150:400–415. <https://doi.org/10.1016/j.psep.2021.04.029>
7. Li T., Chen G., Li Y. et al. Study on Progressive Instability Characteristics of Coal-Rock Composite Structure with the Different Height Ratios. *Geotechnical and Geological Engineering*. 2022;40(3):1135–1148. <https://doi.org/10.1007/s10706-021-01947-0>
8. Serdyukov S., Patutin A., Rybalkin S.L. et al. Directional hydraulic fracturing based on tensile loading. In: *International Multidisciplinary Scientific GeoConference Surveying Geology and Mining Ecology Management – SGEM. International Multidisciplinary Scientific Geoconference*. 2017;17(13):269–274. <https://doi.org/10.5593/sgem2017/13/S03.034>
9. Ingles J., Lamouroux C., Soula J.C. et al. Nucleation of ductile shear zones in a granodiorite under greenschist facies conditions, Neouvielle massif, Pyrenees, France. *Journal of Structural Geology*. 1999;21(5):555–576. [https://doi.org/10.1016/S0191-8141\(99\)00042-5](https://doi.org/10.1016/S0191-8141(99)00042-5)
10. Economides M.J., Mikhailov D.N., Nikolaevskiy V.N. On the problem of fluid leakoff during hydraulic fracturing. *Transport in Porous Media*. 2007;67(3):487–499. <https://doi.org/10.1007/s11242-006-9038-7>
11. Khramchenkov M.G., Korolev E.A. Dynamics of fractures growth in oil saturated carbonate beds of the Republic of Tatarstan. *Neftyanoe Khozyaistvo*. 2017;(4):54–57. <https://doi.org/10.24887/0028-2448-2017-4-54-57>
12. Petrov V.A., Lespinasse M., Poluektov V.V. et al. Rescaling of fluid-conducting fault structures. *Doklady Earth Sciences*. 2017;472(2):130–133. <https://doi.org/10.1134/S1028334X17020027>
13. Matray J.M., Savoye S., Cabrera J. Desaturation and structure relationships around drifts excavated in the well-compacted Tournemire's argillite (Aveyron, France). *Engineering Geology*. 2007;90(1–2):1–16. <https://doi.org/10.1016/j.enggeo.2006.09.021>
14. Andrievskij A.P. Design procedure of optimal parameters of drilling and blasting operations certificate under drilling with straight slot tier cut. *Fiziko-Tekhnicheskie Problemy Razrabotki Poleznykh Iskopaemykh*. 1992;(5):71–76.
15. Kononenko M., Khomenko O., Savchenko M. et al. Method for calculation of drilling-and-blasting operations parameters for emulsion explosives. *Mining of Mineral Deposits*. 2019;13(3):22–30. <https://doi.org/10.33271/mining13.03.022>
16. Krstic S., Ljubojev M., Ljubojev V. et al. Monitoring the stability of the rock mass excavating of underground premises in the ore body t1, jama bor. In: *International Multidisciplinary Scientific GeoConference Surveying Geology and Mining Ecology Management – SGEM. International Multidisciplinary Scientific Geoconference*. 2014;2(1):613–619. <https://doi.org/10.5593/sgem2014/b12/s2.078>
17. Sudarikov A.E., Merkulova V.A. Specifics of calculating the stability of mine workings when applying drilling and blasting. *ARPJ Journal of Engineering and Applied Sciences*. 2017;12(21):6192–6196. URL: https://arpnjournals.org/jeas/research_papers/rp_2017/jeas_1117_6471.pdf
18. Abaturova I., Savintsev I., Korchak S. Assessment of risk of development of contingency situations on railway tracks. In: *Engineering and Mining Geophysics 2018 – 14th Conference and Exhibition. European Association of Geoscientists and Engineers*. 2018. P. 137600. <https://doi.org/10.3997/2214-4609.201800545>
19. Nurpeisova M.B., Kirgizbayeva D.M., Kopzhasaruly K. Innovative methods of the rock massif fractures survey and treatment of its results. *Naukovyi Visnyk Natsionalnoho Hirnychoho Universytetu*. 2016;(2):11–18.
20. Levytskyi V., Sobolevskiy R., Zawieska D. et al. The accuracy of determination of natural stone cracks parameters based on terrestrial laser scanning and dense image matching data. In: *International Multidisciplinary Scientific GeoConference Surveying Geology and Mining Ecology Management, SGEM*. 2017;17(23):255–262. <https://doi.org/10.5593/sgem2017/23/S10.031>
21. Golik V., Stas G., Morkun V. et al. Study of rock structure properties during combined stopping and development headings. In: *The International Conference on Sustainable Futures: Environmental, Technological, Social and Economic Matters (ICSF 2020)*. 2020;166:03006. <https://doi.org/10.1051/e3sconf/202016603006>
22. Tian W.L., Yang S.Q., Dong J.P. et al. An experimental study on triaxial failure mechanical behavior of jointed specimens with different JRC. *Geomechanics and Engineering*. 2022;28(2):181–195. <https://doi.org/10.12989/gae.2022.28.2.181>
23. Fan X., Yu H., Deng Z. et al. Cracking and deformation of cuboidal sandstone with a single nonpenetrating flaw under uniaxial compression. *Theoretical and Applied Fracture Mechanics*. 2022;119:103284. <https://doi.org/10.1016/j.tafmec.2022.103284>
24. Ren S., Han T., Fu L. et al. Pressure effects on the anisotropic velocities of rocks with aligned fractures. *Acta Geophysica Sinica*. 2021;64(7):2504–2514. (In Chinese) <https://doi.org/10.6038/cjg202100318>



25. Anderson I., Ma J., Wu X. et al. Determining reservoir intervals in the Bowland Shale using petrophysics and rock physics models. *Geophysical Journal International*. 2022;228(1):39–65. <https://doi.org/10.1093/gji/ggab334>
26. Wu J., Goto T., Koike K. Estimating fractured rock effective permeability using discrete fracture networks constrained by electrical resistivity data. *Engineering Geology*. 2021;289:166–178. <https://doi.org/10.1016/j.enggeo.2021.106178>
27. Attya M., Hachay O., Khachay O. New method of defining the geotechnical parameters from CSEM (controlled source electromagnetic method) monitoring data at the 15th May City, Egypt. *Methods and Applications in Petroleum and Mineral Exploration and Engineering Geology*. 2021;371–388. <https://doi.org/10.1016/b978-0-323-85617-1.00022-9>
28. Grib N.N., Uzbekov A.N., Imaev V.S. et al. Variations in the geoelectric properties of the rock masses as a result of the seismic effects of industrial explosions. In: IOP Conference Series: Earth and Environmental Science. *World Multidisciplinary Earth Sciences Symposium (WMESS 2019)*. 9–13 September 2019, Prague, Czech Republic. 2019;362(1):012120. <https://doi.org/10.1088/1755-1315/362/1/012120>
29. Sizin P.E., Shkuratnik V.L. Theoretical estimation of microcracks influence on rocks conductivity with maxwell approximation. *Mining Informational and Analytical Bulletin*. 2015;(3):212–218.
30. Landau L.D., Lifshits E.M. *Theoretical physics: At 10 parts. T. VIII. Electrodynamics of continuous media*. Moscow: Fizmatlit; 2005. 656 p. (In Russ.)
31. Bruggeman D.A.G. Berechnung verschiedener physikalischer Konstanten von heterogenen Substanzen. I. Dielektrizitätskonstanten und Leitfähigkeiten der Mischkörper aus isotropen Substanzen. *Annalen der Physik*. 1935;416(8):665–679. (In German) <https://doi.org/10.1002/andp.19354160802>
32. Landauer R. Conductivity of cold-worked metals. *Physical Review*. 1951;82(4):520–521. <https://doi.org/10.1103/PhysRev.82.520>
33. Landauer R. High-field magnetoresistance of point defects. *Journal of Physics F: Metal Physics*. 1978;8(11):L245–L250. <https://doi.org/10.1088/0305-4608/8/11/001>
34. Balagurov B. Ya. *Electrophysical properties of composites: Macroscopic theory*. Moscow: LENAND; 2015. 752 p. (In Russ.)
35. Kasakhara K. *Earthquake Mechanics*. Moscow: Mir; 1985. 264 p. (In Russ.)
36. Shklovskii B.I., Efros A.L. Percolation theory and conductivity of strongly inhomogeneous media. *Soviet Physics Uspekhi*. 1975;18(11):845–862. <https://doi.org/10.1070/PU1975v018n11ABEH005233>
37. Pride S.R., Berryman J.G., Commer M. et al. Changes in geophysical properties caused by fluid injection into porous rocks: analytical models. *Geophysical Prospecting*. 2017;65(3):766–790. <https://doi.org/10.1111/1365-2478.12435>
38. Tan X., Konietzky H. Numerical simulation of permeability evolution during progressive failure of Aue granite at the grain scale level. *Computers and Geotechnics*. 2019;112:185–196. <https://doi.org/10.1016/j.compgeo.2019.04.016>
39. Voznesensky A.S., Kidima-Mbombi L.K. Formation of synthetic structures and textures of rocks when simulating in COMSOL Multiphysics. *Mining Science and Technology (Russia)*. 2021;6(2):65–72. <https://doi.org/10.17073/2500-0632-2021-2-65-72>
40. Zhukov V.S. Influence of intergranular and fractured porosity on the electrical resistivity of reservoirs of the Chayandinsky field (Eastern Siberia). *Geophysical Research*. 2022;23(2):5–17. (In Russ.) <https://doi.org/https://doi.org/10.21455/gr2022.2-1>

Information about the authors

Pavel E. Sizin – Cand. Sci. (Phis. and Math.), Associate Professor of the Department of Mathematics, University of Science and Technology MISIS, Moscow, Russian Federation; ORCID [0000-0001-8156-4972](https://orcid.org/0000-0001-8156-4972), Scopus ID [6506196727](https://orcid.org/6506196727); e-mail sizin.pe@misis.ru

Alexander S. Voznesenskii – Dr. Sci. (Eng.), Professor of the Department of Physical Processes of Mining and Geocontrol, University of Science and Technology MISIS, Moscow, Russian Federation; ORCID [0000-0003-0926-1808](https://orcid.org/0000-0003-0926-1808), Scopus ID [57210211383](https://orcid.org/57210211383), ResearcherID [C-3863-2015](https://orcid.org/C-3863-2015), SPIN 5976-3030; e-mail al48@mail.ru

Lemuel Ketura Kidima-Mbombi – PhD student, Department of Physical Processes of Mining and of Geocontrol, University of Science and Technology MISIS, Moscow, Russian Federation; Scopus ID [57226447408](https://orcid.org/57226447408)

Received 12.07.2022

Revised 08.08.2022

Accepted 15.12.2022